Electromagnetic MEMS Scanning Mirrors

Raanan A. Miller and Yu-Chong Tai

Electrical Engineering , MS 136-93

California Institute of Technology,

Pasadena, CA 91125

We report here a new magnetic MEMS technology that enables many electromagnetic MEMS devices. This new technology combines magnetic thin films and silicon bulk micromachining. Its use is demonstrated by two types of millimeter-sized scanning mirrors that are capable of delivering deflection angles exceeding 60 degrees. Details include the design, fabrication, operation, as well as a complete electromechanical model of the mirrors. In addition, the use of the mirrors is further manifested in a holographic data storage system where hundreds of holograms have been successfully stored and retrieved.

1 INTRODUCTION

Recent developments in silicon micromachining have enabled many novel Micro-Electro-Mechanical Systems (MEMS) [1]. These systems, however, are mainly developed for microsensors with considerably less work done on microactuators. Even among the few works on actuators, the majority of effort has been on electrostatic and piezoelectric actuation. Nevertheless, we think electromagnetic actuation is very promising and magnetic actuation has many advantages over both the electrostatic and piezoelectric actuation. For example, achievable magnetic forces in a microactuator can be both attractive and repulsive. They can also be large in magnitude (~ mN) and effective over a long range (~ mm) [2]. However, the major disadvantage of magnetic actuation is the lack of a mature technology. This is mainly because magnetic actuation requires more complicated components such as coils and magnetic core materials.

Here we then report our efforts to develop a new magnetic MEMS technology, which enables many new magnetic MEMS devices. Our approach is to integrate magnetic thin films with bulk silicon micromachining. As a demonstration, we have developed two types of small size, low cost, highly accurate, large angle-of deflection MEMS laser-scanning mirrors. These devices can be used in many applications ranging from bar-code scanners to scanning mirrors in holographic data storage systems. The two types of actuators are: (1) mirrors with permalloy ($Ni_{90}Fe_{10}$) only, and (2) mirrors with both permalloy and copper coils. Both devices have different advantages and their use depends on the application. The type-1 mirrors can be controlled by an external magnetic field so they don't experience thermal heating effects. The type-2 mirrors also require an external field but can be

controlled using a coil current. This feature is especially useful if individual addressability is necessary when many mirrors are used in an array.

2 DESIGN

The mechanical structure of the permalloy-only (as called type-1) mirror (Fig. 1) consists of a single-crystalline silicon plate (4 x 4 x 0.04 mm³) tethered to the bulk silicon substrate by two serpentine springs. A 3 mm x 3 mm permalloy layer is located on the bottom side of the plate and it is used to induce the magnetic actuation. An additional permalloy mesh structure sits on the top side of the plate and constrains the mirror with deflections only above the substrate. Here the top surface of the plate framed by the mesh is the mirror reflector. The type-2 mirror design then includes a 30 turn copper coil in addition to the permalloy layer. This mirror (Fig. 2) has the same silicon plate and springs as the type-1 mirror but its bottom mirror-like surface (single-crystalline silicon) serves as the reflector and on its top surface sit the 30-turn copper coil and the thin-film permalloy layer. Both the coil and permalloy can be used to provide the actuation forces.
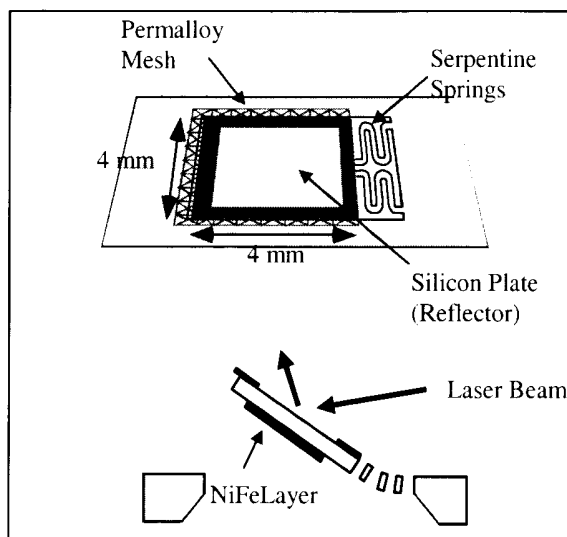

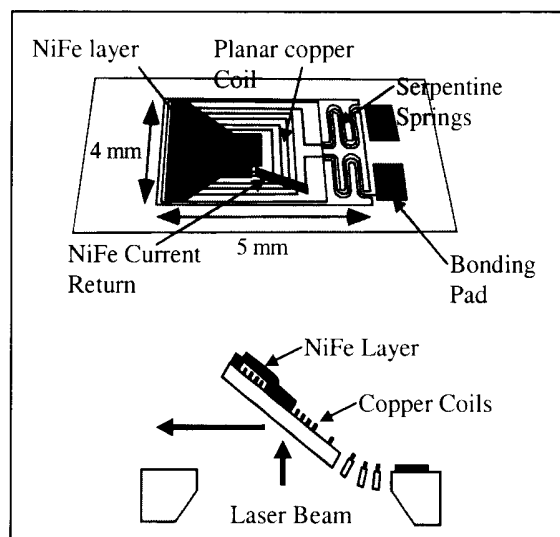**Figure 1**: Schematic top view and cross-sectional view (deflected) of permalloy only (type-1) mirror

Figure 2: Schematic top view and cross-sectional view (deflected) of type-2 MEMS mirror.

3 FABRICATION

The fabrication steps for the type-1 mirror (Fig. 3) start with the bulk micromachining of a 40 μm thick epitaxial silicon membrane by anisotropically etching the bulk silicon down to a boron etch-stop layer. The boron layer is then removed and an oxide layer is grown. A Ti/Cu seedlayer is next evaporated on the bottom side of the silicon plate. A photoresist mold is formed and 20 μm of permalloy is deposited. The photoresist and seedlayer are then removed. Next a Ti/Cu seedlayer is evaporated on the top side of the mirror, and a 10 μm permalloy mesh structure is electroplated. This mesh extends beyond the intended (4 mm x 4 mm) border of the plate. The mirror is then freed from the substrate in two steps. First, in the areas outside the plate region the permalloy mesh is detached

from the silicon substrate by etching away the oxide layer with an HF etchant. Then, the plate and springs are lithographically patterned on the membrane, free-released by reactive-ion-etching (RIE). In this RIE step, the silicon under the permalloy mesh is also etched so as to free the mirror from the substrate. The mesh remains overhanging the edge of the freed plate, and serves two purposes. First it constrains the mirror to deflections above the plane. Second, the mesh improves the shock resistance of the mirrors, which allows mirrors with softer springs (hence larger deflections at lower magnetic fields). Finally, a thin (200 nm) layer of aluminum is evaporated on the top reflector to serve as the mirror surface.
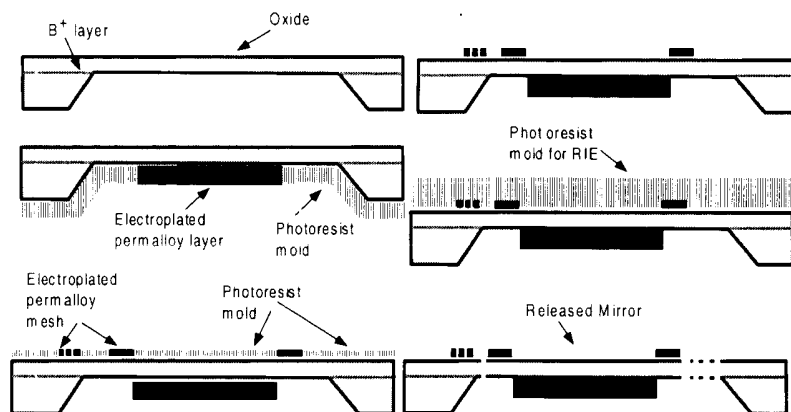

Figure 3: Schematic showing key type-1 mirror fabrication steps

The fabrication steps for the type-2 mirror (Fig. 4) also involve the formation of a 40 µm membrane as described previously. A Ti/Cu seedlayer is however evaporated on the top side of the plate. A photoresist mold is formed and a 30-turn planar copper coil is electroplated (9 µm thick). Next an insulating photoresist layer is coated, patterned and hard-baked. A Ti/Cu seedlayer is again evaporated, a photoresist mold is formed and an 11 µm thick permalloy layer electroplated. Here, a small piece of permalloy (as shown in Fig. 2) serves as a current return path when current is provided to the coil. Finally a thick layer of photoresist is coated and the spring and plate structures are photo-lithographically defined. The exposed oxide layer is removed in BHF and the silicon beneath is reactive-ion-etched to free-release the mirror.
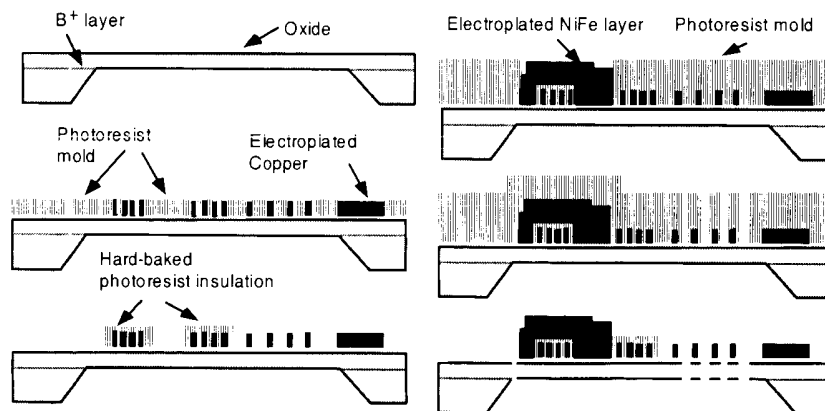

Figure 4: Schematic type-2 mirror fabrication steps

4 MIRROR OPERATION

The are two modes of magnetic actuation used in our mirrors. The first one is the permalloy actuation, and the second mode is the coil actuation. The permalloy actuation can be applied to both types of mirrors but coil actuation applies to type-2 mirrors only. The following gives a detailed description of both types of actuation.

4.1 Permalloy Actuation

Mirror deflections (Figs. 5 & 6) for both mirror types can be produced by interaction between an external magnetic field and the magnetic moment in the NiFe layer, as called permalloy actuation. The external magnetic field first induces a magnetic moment in the NiFe and the interaction between the magnetic field and the permalloy magnetic moment produces a torque in the direction to align the moment with the field direction. In the case of a non-uniform magnetic field, a translational force that is proportional to the gradient of the magnetic field will also be produced (as shown in Fig. 7). In our experiments, though, magnetic modeling of the mirror actuation is investigated in a uniform magnetic field, H_{ext}. The magnetic field is perpendicular to the wafer surface and an out-of-plane rotation of the plate is induced. The deflection angle for each mirror is then measured at different field strengths and is shown in Fig. 8.
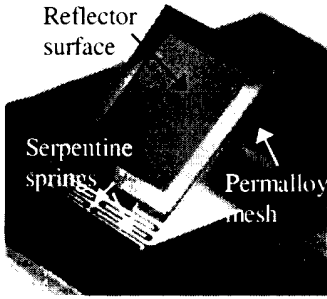

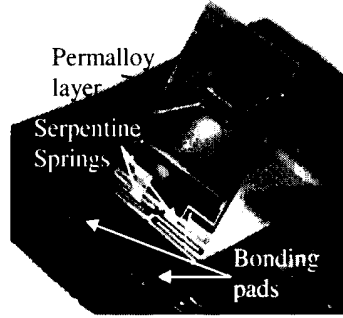**Figure 5**: Photograph of actuated type-1 MEMS mirror

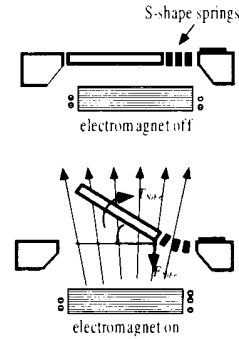**Figure 6**: Photograph of actuated type-2 MEMS mirror

Figure 7: Schematic of mirror actuation concept

The deflection for both mirrors is modeled using the torque balance (Fig. 9) between the permalloy torque (T_{NiFe}) and the restoring torque of the spring (T_{spring}). The permalloy torque T_{NiFe} (also described in literature [3,4]) is produced by the interaction between B_{ext} and a magnetic moment m_{NiFe} in the permalloy

$$T_{NiFe} = | m_{NiFe} \times B_{ext} | = V_{NiFe} M_{NiFe} H_{ext} \sin(90 - \theta) \quad (1)$$

where $V_{NiFe} = 7.26 \times 10^{-11}$ m^3 is the volume of the permalloy, H_{ext} is given in A/m, θ is the deflection angle of the flap relative to the substrate and M_{NiFe} is the magnetization of the permalloy induced by $H_{ext} \cos(90 - \theta)$. The torque (in N-m) is then counterbalanced by the restoring torque of the spring as

$$T_{spring} = K \theta \quad (2)$$

where $K_1 = 9.2 \times 10^{-8}$ Nm/deg, $K_2 = 4.2 \times 10^{-8}$ Nm/deg are the measured torsional spring constants for the type-1 and type-2 mirrors respectively, and θ is the deflection angle of the mirrors. Eqs. 1 and 2

are the governing equations for the operation of the mirrors as shown in Fig. 8, where the theory (solid and dashed lines) fits the experimental data very well. Note that the necessary information of $M_{NiFe}(H_{ext})$ was determined experimentally by BH-loop and vibrating sample magnetometer (VSM) measurements performed on the permalloy layer of each particular mirror [5]. The B-H loop gives the shape of $M_{NiFe}(H_{ext})$, while the VSM measurement determined the saturated magnetization (M_s), which is 0.79 Tesla for the type-1 mirrors and 0.78 Tesla for the type-2 mirrors.
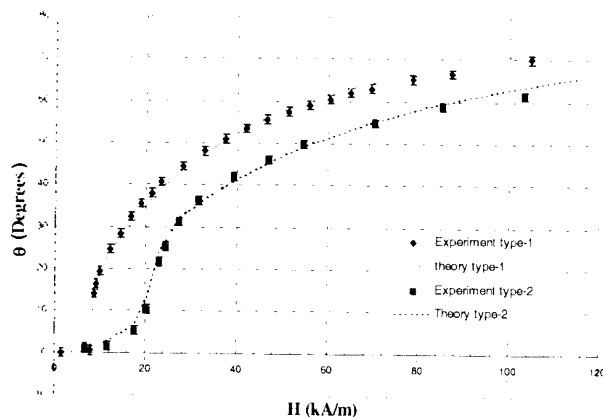

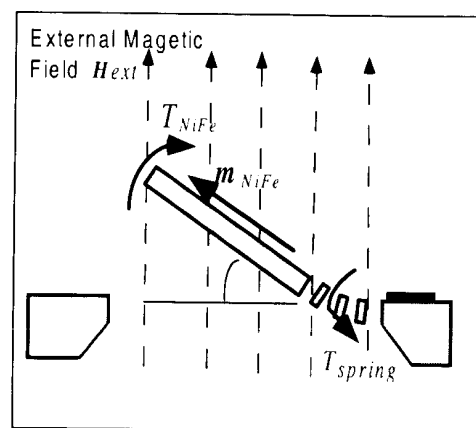**Figure 8**: Deflection angle of type-1 and type-2 MEMS mirrors vs. External magnetic field.

Figure 9: Torque balance of the mirror with permalloy only in an external magnetic filed.

4.2 Coil Actuation

Coil actuation comes from the interaction between an external magnetic field and a electrical coil with a flowing current. The type-2 mirrors can be operated in this coil-actuation mode, where an applied current to the on-plate coils (in the presence of a magnetic field) can control the mirror deflection angle. For type-2 mirrors, a constant external magnetic field will first cause a permalloy flap to deflect to a fixed "bias" angle due to the permalloy-actuation. Deflection about this position can then be further controlled by changing the magnitude and direction of the current supplied to the coils. A convenient way of controlling a type-2 mirror is then to use the external field for coarse deflection control and to use the coil current for fine positional control. This operation has been experimentally explored and Fig. 11 shows the coil-actuated deflection angle of a type-2 mirror in an external bias field set to 79 kA/m (994 Oe). Without the coil current, this magnetic field saturates the magnetic moment in the permalloy and then causes a bias angle $\theta = 58°$ due to permalloy actuation.
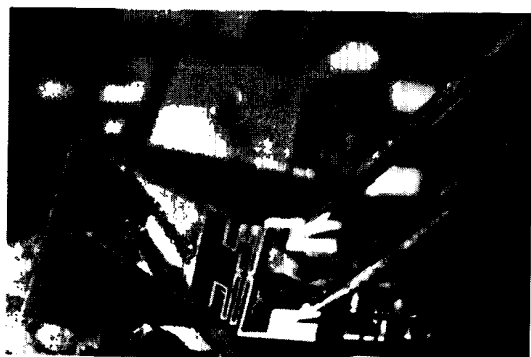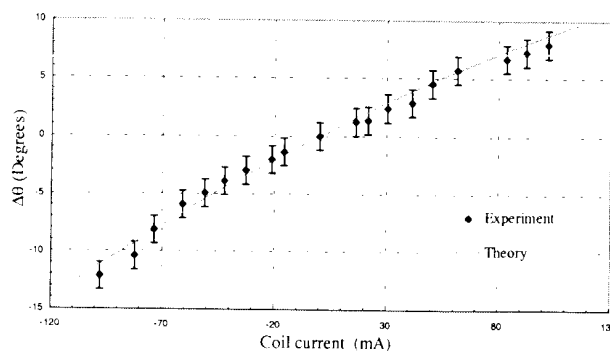

Figure 10. Actuated mirror in an external field

Figure 11. Change in deflection angle from "bias"

(Hext = 23.9 kA/m (300 Oe) vertical to the substrate) with a coil current of around 30 mA. The deflection is caused by both the permalloy and coil current.

position variable coil current with external field of 79 kA/m (994 Oe).

To model the coil actuation (as in Fig. 11), we add two more terms, T_{coil} and $T_{thermal}$, in the torque balance equation (as shown in Fig. 12). The T_{coil} term is the torque induced from a current moment, $m_{coil} = I A_{total}$, in a magnetic field given as

$$T_{coil} = |m_{coil} \times B_{ext}| = m_{coil} B_{ext} \sin \theta \qquad (3)$$

where I is the current supplied to the coils in amps, $A_{total} = 0.000132$ m^2 is the sum of 30-turn areas, and $B_{ext} = \mu_o H_{ext}$ is the magnetic flux density in Tesla. On the other hand, the thermal torque is induced by heat generated by this current flowing in the coils. This is modeled by

$$T_{thermal} = -C I^2 \qquad (4)$$

In this case $C = 25.2 \times 10^{-6}$ Nm/A^2 is a fitting parameter while I is the applied coil current in amps. The negative sign in Eq. 4 means that the thermal torque always bends the mirror down. As a result, when a current is applied to the coils with a constant external magnetic field, the torque balance equation then becomes

$$V_{NiFe} M_s H_{ext} \cos \theta + m_{coil} B_{ext} \sin \theta - C I^2 = K \theta \quad (5)$$

Fig. 11 then shows both the experimental and theoretical data of a type-2 mirror controlled by the coil actuation. The theory is shown in the solid line and a good fit is obtained. Note that Fig. 11 also shows that the coil actuation can produce a $\pm 10°$ deflection which is useful for scanning mirror applications.
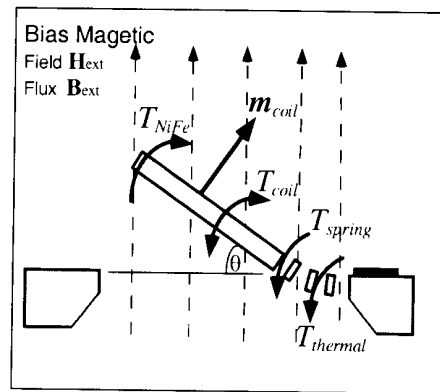

Figure 12. Torque balance of the mirror with both the permalloy and coil current in an external magnetic field.

5 MIRROR QUALITY

For the type-1 mirror, the actuating permalloy layer is located on the bottom side of the plate. We design it this way so the top original silicon surface is used as the mirror surface with an excellent

surface roughness less than 10 nm over the entire mirror. However, the slight stress in the permalloy layer does cause the mirror become slightly convex. This curvature actually depends on the magnetic field. While the measured horizontal radius of curvature is a constant of 7.5 cm, the vertical radius of curvature varies from 20 to 25 cm corresponding to a magnetic field 0 - 20 kA/m. For thinner permalloy layers the radius of curvature becomes larger (> 75cm for 5μm thick permalloy) but did not change with field strength.

For the type-2 mirror, the top side of the mirror is used to place the permalloy and coils so the bottom side of the silicon plate is the reflector. The bottom surface is then slightly rougher (~ 45 nm) because we used an epitaxy wafer in our process. It is found that this mirror is also convex with a curvature radius of 1 cm. Interestingly though, we observed no change in radius of curvature at field strengths up to 23 kA/m (300 Oe). Nevertheless, if necessary, the surface roughness and the warpage of the mirrors can both be easily improved using silicon-on-insulator (SOI) wafers. For our use of the mirrorsin laser holographic data storage, the imperfection of the mirror is not important. As long as the reflected beam off the mirror for a given angle is consistently reproducible, good quality holograms can be written and retrieved as demonstrated in the following.

6 HOLOGRAPHIC DATA STORAGE

In general, volume holographic data storage is achieved by using two laser beams (one reference beam and one signal beam) which interfere with each other and form a 3-D interference pattern (hologram) in a light-sensitive crystal (such as Fe-doped $LiNbO_3$) that "memorizes" it. In this process, the interfering beams change the optical properties of the crystal and the crystal stores this 3-D interference grating. To read the data, only the reference beam is needed to shine through the crystal and the pre-stored 3-D grating inside the crystal reproduces the signal beam [6]. Holographic memory systems with both large capacity and rapid access require high-speed wide-angle beam steering elements. Mechanically rotated conventional mirrors or acousto-optic deflectors were commonly used in experiments. These devices are bulky, expensive, and introduce noise through either pointing inaccuracy or wavefront distortion. An emerging deflector technology is based on liquid crystals. However, devices with a large number of deflection angles are difficult to fabricate. Here we report the results on the first use of MEMS mirrors in holographic storage. These devices potentially offer low cost, low mass, and large scanning angles.

6.1 Type-1 MEMS mirror

Using the setup shown in Figure 14a, we demonstrated the type-1 mirror as a deflector for angle multiplexed holographic storage. The mirror is placed on a solenoid-type electromagnet, which is driven by a DC voltage regulator to generate the desired magnetic field. In this system configuration a single laser beam (Argon laser) is split into a reference beam and a signal beam path. The latter contains an information presentation device (Liquid Crystal Display), a storage crystal, and a detector (CCD camera). The reference beam, is deflected by the MEMS mirror and then passes through a lensing system. The lenses keep the beam focused on the same location on the crystal but with different incident angles corresponding to the mirrors deflection angle. The volume nature of the holograms allows a page of data to be stored for each different deflection angle, provided that these angles are sufficiently separated. In this demonstration, we stored 100 holograms using the type-1 mirror. Some hologram reconstruction's are shown in Figure 13. The holograms are of good quality

except that the evident concentric circles are an artifact of the crystal surface not being polished well. Although each hologram was spaced from its neighbor by 0.143°, much smaller deflections (0.007°) were generated with the mirror and the control circuit used. Practically, many more holograms can be stored although we have demonstrated only 100 of them.

In this experiment we found that to improve the mirror response time the mirror should be deflected in small angular steps by incrementally providing additional current to the electromagnet until reaching the desired mirror deflection angle. These small angle increments minimize the over-shoot and produce an overall faster mirror response. As an example, a deflection of 10.7 ° (0.187 rad), incremented in steps of 0.7 ° (0.012 rad), could be performed in ~ 200 milliseconds. If the 10.7 ° jump was executed in one step the mirror would ring for more than 400 milliseconds. We also investigated how accurately the mirror could return to a specific deflection angle. The type-1 mirror was deflected from 0 to 53 ° more than 20 times. Each time we found that the mirror returned to within 0.003 ° (64 μrad) of the 53 ° deflection angle. Finally, the angular stability of the mirrors was also measured when the mirror was deflected to 53 ° any change from the deflection angle over a 5 minute period was noted. The measured angular fluctuation of this mirror was less than 0.0006 ° (10 μrad).

Figure 13: Four random holograms stored and retrieved using the type-1 mirror.

6.2 Type-2 MEMS mirror

In the holographic data storage demonstration using the type-2 mirror, the mirror is first biased to approximately 45° in a constant but non-uniform external field (~200 Oe at mirror), provided by a permanent magnet located 2mm above the surface of the mirror. Deflections about this angle (fine control), are induced by varying the coil current. Two multiplexing schemes are explored. First the type-2 mirror is used in the same angle multiplexing storage system that the type-1 mirror was used in (Fig. 14a). The same success has been obtained and Fig. 15 shows some typical holograms stored and then retrieved using the MEMS scanning mirror. In addition to the angular multiplexing scheme, the mirror is also used in a combined spatial/angular multiplexing configuration (Fig. 14b). Here, not only is the incident angle of the reference beam changed but so is its position on the crystal.   The primary advantage of this configuration is that two lenses can be eliminated and the mirror placed right at the crystal surface. Once again for demonstration purposes we stored 100 holograms, all were of good quality.

Fixed angular increments of ~ 0.3 ° (5 mrad), for the type-2 mirror, were found to provide the shortest time to reach and settle on a particular hologram. Each 0.3 ° angle increment took ~ 25 milliseconds. In future work we plan to investigate other methods to improve the mirrors response. Some possibilities include increasing the mechanical damping of the springs by coating them with lossy materials such as polyimide, increasing the spring stiffness, or shaping the driving input signals so as not to excite resonant modes. The type-2 mirror (magnetic field fixed and current supplied to the

coils) returned to within 0.002 ° (40 µrad) when the mirror was deflected multiple time in this case from 0 to 2 °. Once the mirror was deflected to the above deflection angle its angular stability was also measured. Any change from the above deflection angle over a 5 minute period was noted. Angular fluctuation for this mirror was less than 0.0006 ° (10 µrad).

As a conclusion, the MEMS mirrors are an attractive angle-multiplexing technology for holographic data storage. They possess a very large continuous deflection range, are compact, and use only moderate power. Though the two types of mirrors performed equally well in their ability to store and retrieve holograms, in terms of operational versatility the type-2 mirror may be more advantageous.
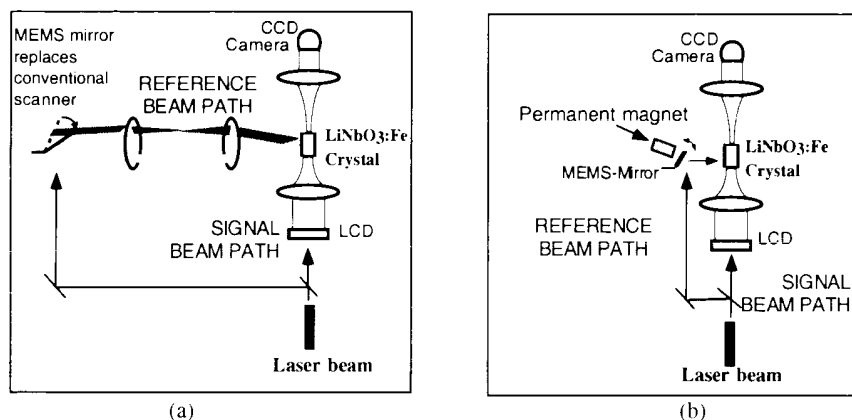

(a)   (b)

Figure 14. (a) Conventional holographic storage system using commercial beam deflectors.
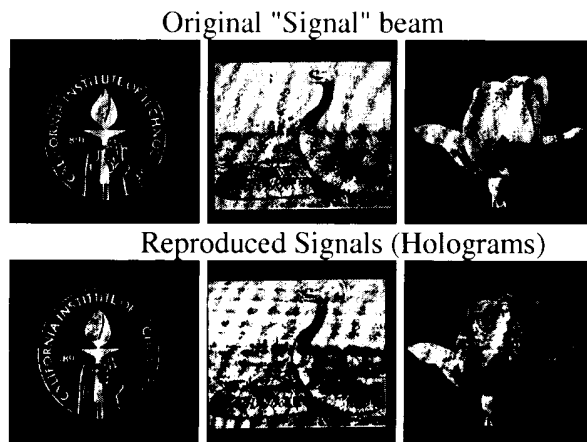(b) Compact storage system with MEMS mirror.

Figure 15. Holograms stored and retrieved, showing original image prior to storage and retrieved image from crystal.

7 DISCUSSION

From a technological point of view, several new issues arise from the incorporation of magnetic thin film materials into silicon bulk micromachining. Magnetic forces in microactuators are

proportional to the volume of magnetic material. Therefore micro-actuators generally require thicker layers of magnetic material than those used in thin film recording heads if a large magnetic force is desired. This, however, introduces stress and adhesion problems. Also, care must be taken that the thermal cycling or chemical etching used in the micromachining process do not damage the magnetic materials. Finally, magnetic properties such as remnant magnetization, saturation field, and coercivity of the films may need to be optimized for the specific requirements of the device.

For evaluation purposes a comparison of the MEMS mirrors with some commercial scanning devices is provided in Table 1. Although the indicated hologram spacing for the commercial devices is better than the MEMS mirrors the objective has been simply to demonstrate that the storage of ~ 100 holograms using the MEMS mirrors is practical. Future work is planned to determine how closely , in angle, these holograms can be spaced using the MEMS mirrors. On the other hand, the deflection range for both MEMS mirrors is larger than either of the commercial devices. To reduce thermal effects due to current heating in the type-2 mirrors the current induced deflection range of 20° can be reduced while incorporating the external coarse control. The time response of the MEMS mirrors is significantly better than the commercial motorized stage but worse than that of the acousto-optic deflector. Mirror response times can be further improved by increasing the resonant frequency of the mirrors (compromising some of the large deflection range) or increasing mechanical damping, e.g., by coating springs with polyimide. From Table 1 it is apparent that using the MEMS mirrors does significantly reduce the overall volume of the demonstrated holographic storage system. To further improve storage capacity, future work may include a design for a multi-MEMS-mirror array storage system.

Device	MEMS type-1 mirror	MEMS type-2 mirror	Commercial Motorized stage	Acousto-optic Deflector
Achieved hologram spacing	0.143°	0.03°	0.002°	0.0015°
Deflection range	60°	60°	35°	1.5°
Access time for 0.3° deflection	33 msec	25 msec	130 msec	70 μsec
Reference beam path volume*	100 cm³	1 - 10 cm³ **	686 cm³	1372 cm³
Device volume	5 cm³	1 cm³	60 cm³	30 cm³
Cost	Potentially low	Potentially low	Expensive	Expensive

* Not including laser.
** For compact configuration as in Fig. 14b.

Table 1. Comparison of MEMS mirror with two commercial scanning devices

8 CONCLUSION

Large angle of deflection scanning MEMS mirrors have been successfully developed. The operation of mirrors with permalloy only and mirrors combining permalloy and coils have been modeled and good agreement is found between theory and experiment. Significant reduction in holographic system volume is achieved using the mirrors. Finally, the mirrors have been successfully

demonstrated in a holographic storage application demonstrating the feasibility of combining bulk micromachining with magnetic thin film actuation technology.

9 ACKNOWLEDGMENT

REFERENCES

1. J. Bryzek, K. Petersen, "Micromachines on the march", *IEEE spectrum*, 20 -31 (1994).

2 . C. Liu, T. Tsao,Y.C. Tai et.al, "A Micromachined Permalloy Magnetic Actuator Array for Micro Robotics Assembly Systems", *Proceedings of the 8ᵗʰ International Conference on Solid-State Sensors and Actuators (Transducers 95)*, Vol 1, 328-331 (1995).

3. J. W. Judy, R. S. Muller, "Magnetic microactaution of torsional polysilicon structures", *Proceedings of the 8ᵗʰ International Conference on Solid-State Sensors and Actuators (Transducers 95)*, Vol 1, 332 - 335 (1995).

4. C. Liu, T. Tsao, Y.C. Tai, J. Leu, et. al, "Out-of plane permalloy magnetic actuators for delta-wing control", *Proceedings MEMS 95*, 328-331 (1995).

5. R. A. Miller, G. W. Burr, Y.C. Tai, D. Psaltis, C.M. Ho and R. Katti, " Electromagnetic MEMS scanning mirrors for holographic data storage," *Proceedings of Solid-State Sensor and Actuator workshop, Hilton Head*, 183-186 (1996)

6. D. Psaltis and F. H. Mok, "Holographic Memories", *Scientific American*, **273**(5), 70-75 (1995).

Biographies:

Raanan A. Miller received his BS degree in Electrical Engineering from Boston University in 1990, and his MS from the California Institute of Technology in 1992. Currently he is completing his PhD at Caltech developing electromagnetic MEMS actuators.

Yu-Chong Tai received his Ph.D in Electrical Engineering from the Departement of Electrical Engineering of University of California at Berkeley in 1989. After Berkeley, he joined the faculty of electrical engineering at the California Institute of Technology (Caltech), where he is currently an Associate Professor. Dr. Tai's major research has been micromachining for solid-state microsensors and microactuators (or MEMS) since his Ph.D education. At Berkeley, he was the inventor of the first electrically-spun polysilicon micromotor. At Caltech, he has built a micromachining laboratory and a program of about 15 researchers. His current research interests include new MEMS technologies and devices such as shear-stress sensors, pressure sensors, culture neuron probes, micro fluidic devices, micromotors for hard-disk drives, microphones, magnetic microactuators, and MEMS systems for active fluid control. Because of his research, he has received several awards such as the IBM fellowship, the Best Thesis Award, the presidential Young Investigator (PYI) Award and the David and Lucile Packard Fellowship. He is also a member of the editorial board of the Journal of Micromechanics and Microengineering.